Electronic Supplementary Material (ESI) for Nanoscale.
This journal is © The Royal Society of Chemistry 2019

Supplementary information

Conformation switching of single native proteins revealed by nanomechanical probing without a pulling force

Fabiola A. Gutiérrez-Mejía [†,‡], Christian P. Moerland[†,‡], Leo J. van IJzendoorn [†,‡], Menno W.J Prins[*, †,‡,§]

[†]Department of Applied Physics, Eindhoven University of Technology (TU/e), Eindhoven, the Netherlands

[‡] Institute for Complex Molecular Systems (ICMS), TU/e, Eindhoven, The Netherlands,

[§] Department of Biomedical Engineering, TU/e, Eindhoven, the Netherlands

Index

S1. Materials and Methods

In this section details of sample preparation and data acquisition procedures are described

Particle functionalization. Commercially available carboxylic acid superparamagnetic M-270 particles (2.8 μm diameter, ThermoFisher) were used with the standard functionalization procedures supplied by the manufacturer. In particular, we used 1-Ethyl-3-(3-dimethylaminopropyl, Sigma Aldrich) carbodiimide (EDC) to form amide bonds between the carboxylic groups of the particles and the primary amino groups on the proteins of interest. First, $10\ \mu L$ of a stock solution of 20 mg/mL of M-270 particles were incubated for 30 min in 200 μL of 8 mg/mL solution of EDC. Thereafter 0.16 mg/mL of antibodies specific for TnI (Cat #4T21, Hytest, MAb 625 for H4, MAb 560 for H2) were diluted in 100 µl of 15 mM of Morpholino Ethanesulfonic acid (MES) buffer (pH 5, Merck). Also, 100 µL Streptavidin (Merck) was diluted in MES buffer to a concentration of 0.03 mg/mL. M-270 particles were incubated for 2 hours with 100 μL of streptavidin and 100 μL of the antibody solutions mentioned above at room temperature. Afterwards, the magnetic particles were magnetically separated and rinsed three times with a wash buffer consisting of TBS (Sigma Aldrich, 100 mM Tris HCl and 150 mM NaCl and 0.1% Tween 20) for 30 minutes. Prior to the experiments, 40 μL of the particle solution was diluted with 4 μL of 200 nm biotin labelled fluorescent nanoparticles (Fluospheres) in 100 μL of wash buffer.

Particle based assay in a closed cell and in a buffer exchange cell. Polystyrene coverslips (Agar Scientific) were cleaned with sequential sonication in baths of isopropanol and ultrapure water for 15 minutes each. To form the assay volume, a circular double-side adhesive tape spacer (Secure seal) was attached to a coverslip. On the circular surface area, 100 μL of 10 nM H1 anti-TnI antibody (Cat #4T211 MAb 19C7, Hytest) solution was incubated for one hour at room temperature. After gently rinsing, the inactive surface was blocked with 100 μL of a 1% solution of Bovine Serum Albumin (BSA, Sigma Aldrich) diluted in TBS during one hour. Then the coverslip was rinsed with TBS, and 100 µL of 30 nM troponin ICT complex (Cat #4T211 8T62 ICT, Hytest) diluted in a calcium rich buffer (100 mM KCl, 10 mM (hydroxymethyl)aminomethane (Tris), 1 mM ethylene glycol tetraacetic acid (EGTA) and 5 mM $CaCl_2$) was incubated for two hours at 4 °C. After the troponin complex was bound to the antibodies, further non-specific interactions were prevented by a second incubation with BSA solution. Thereafter 8.5 μL of the coated magnetic particles diluted in buffer (100 mM KCl, 10 mM Tris, 1 mM EGTA, and with the desired concentration of $CaCl_2$) were sedimented on the assay surface under the influence of a weak (2 mT) magnetic field during 7 min, in order to form the antibody-cTn-antibody sandwich bonds. Thereafter a second clean coverslip was applied to close the fluid chamber. Finally, the fluid chamber was turned upside down, so that gravitational forces could pull the unbound particles from the surface.

For experiments with buffer exchange, the abovementioned protocols were followed but the spacer tape was replaced by a 358 µL RC-20 fluid chamber (Warner Instruments). To seal the chamber, Silicone Grease Kit (111-kit, Warner Instruments) was used according to the product specifications. Buffer was exchanged by a flow of 20 $\mu L\ min^{-1}$ during 1 hour, using a Pump 11 Picoplus syringe pump (Harvard Apparatus) connected to the chamber. The assay buffer consisted of 1% BSA diluted in 100 mM KCl, 10 mM Tris, 1 mM EGTA and the desired concentration of $CaCl_2$ (1 mM or 1 nM). The measurements started with 1 nM $CaCl_2$, followed by flushing with 1 mM $CaCl_2$, and thereafter reflushing with 1 nM $CaCl_2$. A similar buffer exchange protocol has been previously described. [1]

Particle imaging and counting. Particles were imaged using a microscope (DM6000M; Leica Microsystems) with a water-immersion objective and a total magnification of $126x$. The microscope was provided with a high-speed high-resolution sCMOS camera (Andor Neo). The pixel size in the images was 51.6 nm. Images were acquired at $\sim 18\ fps$. Acquired images were analysed with software scripts written in Matlab.

Angular tracking. The angular position of the magnetic particle was measured as a function of time in the MT (large angles) and ABM (small angles) measurements. The angular analysis script uses the first image of the time series as a template. The template consists of a black background with a white ring, without a centre peak. The white ring has the size of the first diffraction ring and has angular perturbations at the positions of the fluorescent labels attached to the particle, see Fig. 1d. The template image and the subsequent centred images are translated into polar coordinates and are then cross-correlated. The position of maximum cross-correlation is used to calculate the angle of rotation. The accuracy of the measured angles has been estimated to be $\pm 1\ deg$, estimated from the capability of the software to find the same value back after the input was deliberately perturbed.

Magnetic Tweezers (MT). Prior to angular deformation, the particles were incubated in a constant magnetic field of 2 mT parallel to the sample surface in order to align the magnetic anisotropy axes of the superparamagnetic particles with the equilibrium position of the protein torsional spring. A four-pole electromagnet with soft-iron cores was used to generate the magnetic torque and consequential particle rotation. Details of the setup have been described by Janssen et al.[2] The magnet has been designed with slanted pole tips in order to generate extremely low vertical field gradients and thereby avoid the application of force. In an MT experiment, a continuously rotating in-plane magnetic field with an amplitude of 20 mT at a frequency $f = 0.5\ Hz$ was applied, first in clockwise and thereafter in counter-clockwise direction for ~5 seconds each. In Ref. [3] the magnetic torque applied by the M-270 particles was determined to be equal to $(2.5 \pm 0.6) \times 10^2\ pNnm$. We quantified the torsion constant from the maximum angle of deformation θ_{max}, calculated as the difference between the maximum angles for clockwise and anticlockwise rotation divided by two. The error in the angle is determined from multiple oscillations. Assuming a linear relationship between angular deformation and applied torque (i.e. a Hookean torsion spring), the maximum angular deformation θ_{max} relates to the torsion constant k averaged over the two senses of rotation by the following relationship:

$$\theta_{max} = \frac{\tau_{m,max}(B)}{k} \qquad (1)$$

Here, the maximum magnetic torque $\tau_{m,max}(B)$ has been experimentally determined by quantifying the maximum rotation frequency of particles free in solution.[3] The oscillatory behaviour of a particle bound by a nanomechanical molecular complex is described in more detail in the SI Section S3.

Angular Brownian Motion (ABM). The ratio between the thermal energy and potential energy originating from the torsional spring determines the probability to find the particle at a certain angle from its equilibrium position. Approximating the torsional spring as a harmonic oscillator, the shape of the angular distribution $P(\theta_p)$ function becomes:

$$P(\theta_p) \propto exp(-\frac{k(\theta_p - \theta_o)^2}{2k_B T}) \qquad (2)$$

where k_B is the Boltzmann constant, T is the temperature, θ_p is the angular position of the particle with respect to the initial position θ_0, and k the torsion constant of the molecular bond. The full width at half maximum ($FWHM = 2.355\sigma$) of the distribution is used as a parameter to measure the angular flexibility, with σ the standard deviation of the distribution. By fitting the distribution, k can be obtained. Experimentally, to avoid a remnant field due to a remnant core magnetization, a demagnetization step was applied prior to the ABM measurement. The demagnetization consisted of driving a sinusoidal current trough two facing coils in the electromagnet with a decreasing amplitude over time. Brownian angular fluctuations were recorded for 120 seconds at $18\ fps$. From the angular time traces, a histogram of the angular positions was obtained, see Figure 2b.

Tethered Particle Motion (TPM). From the particle tracking video, the xy-coordinates of the centre of the particle were determined in absence of a magnetic field. The centre was positioned with subpixel resolution by using the centre of intensity of a subset of pixels in the middle of the particle, see Figure 1d. The displacement of the particle was calculated by correlating the subsequent images with the first image of the series. An effective area A was determined from the centre positions accumulated over time (120 s), where the area was defined to include 95% of the total number of points. We cannot directly relate the amplitude of motion to an effective length of the protein complex due to the inherently compact structure of the protein complex which most likely limits its motion. Moreover, due to the relatively long exposure time of 50 ms per frame (chosen to optimize the precision of angular tracking) motion blurring occurs which gives a reduction of the measured excursion area, see SI Section S4.

S2. Particle bonding analysis

The experimental conditions were optimized to reach the single molecule regime, by incubating a low concentration of the H1 antibody on the polystyrene coverslips, see Fig. S1.

In particle-based immunoassays, the bonding between particles and substrate can have a specific as well as a non-specific origin. Specific interactions are caused by attachment through single or multiple antibody-protein-antibody bonds and the non-specific bonds arise from imperfect blocking of the surfaces[4]. Previous experiments on a cTn sandwich immunoassay using magnetic tweezers[5] yielded the dissociation rates by subjecting the bound particles to magnetic pulling forces. The force dependent dissociation curves revealed the existence of two distinct cTn-dependent bond types, namely a weak bond attributable to non-specific binding of cTn, and a strong bond attributable to single specific antibody–cTn–antibody assemblies.

The data in Fig. S1 show an increase of the specific particle binding at 1 nM concentration and higher. In the experiments of this paper, a 10 nM concentration of H1 antibody was used, as this optimized the number of particles with specific bonds.

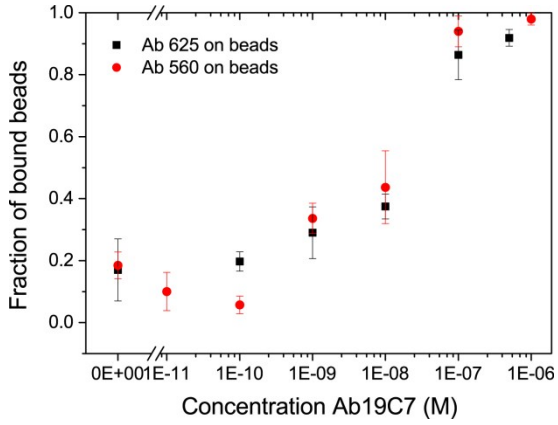

Figure S1. *Fraction of antibody-coated magnetic particles bound to a polystyrene surface that was provided with H1-cTn. The H1 antibodies were incubated on the polystyrene surface at the concentration indicated on the x-axis, followed by incubation with cTn and blocking with BSA (see Methods). Thereafter the surface was incubated with magnetic particles, which were provided with anti cTnI H4 (black squares) or anti cTnI H2 antibodies (red dots). After 10 minutes of incubation, the samples were sealed and turned upside down, thereafter a fraction of particles sedimented (=unbound fraction) and a fraction remained attached (=bound fraction). The data show the fraction of bound particles as a function of the concentration of anti cTnI H1 incubated on the polystyrene substrate.*

S3. Quantification of the torsion constant using simulations

From the rotational movement of the particle, the torsional properties of the molecular complex can be inferred. Previous experiments on Protein G–IgG and IgG–IgG,[3] showed that single specific bonds correspond to particles exhibiting a regular oscillatory behaviour in a rotating field, and that non-specific bonds give immobile or continuously rotating particles. In the present experiments, we observe three different fractions of particles: continuously rotating particles~70%, oscillatory particles ~10%, and immobile particles ~20%. We focus on the population of oscillatory particles as these represent the specific single bonds. Furthermore, all data shown in this paper is from oscillatory particles that did not detach and that remained bound to the substrate during the complete experiment (~90 min).

The measurements of the molecular architectures under continuous torsional deformation describe a sawtooth-like behaviour with an amplitude of oscillation that is nearly constant over the actuation time. The sawtooth frequency equals twice the frequency of the applied magnetic field, which is caused by a remagnetization of the magnetic particle, as was demonstrated an earlier study.[3] The clockwise and anticlockwise sawtooth traces show differences in amplitude, see Figure 2a. The maximum angle of oscillation compared to the equilibrium position (horizontal baselines in Figure 2a) as well as the peak-to-peak distance depend on the sense of rotation. We attribute the differences to a skewness of the angular potential of the molecular complex. The skew may be caused by a non-rotational symmetry around the probing axis, therefore the torsional stiffness of the molecular complex depends on the deformation direction, see Fig. S2. The asymmetry may originate from the inherent non-rotational symmetry of cTnI and/or non specific absorption, but also the orientations of the immobilized antibodies may play a role. The maximum angle of deformation $2\theta_{max}$ was obtained from the data by taking the difference between the maximum angles for clockwise and anticlockwise rotations (see Fig.2a) and is used as a readout parameter for the rotational mechanical stiffness of the targeted region of the troponin complex.

In this section the behavior is described of a superparamagnetic particle bound to a surface by a protein torsional spring. When exposed to a continuously rotating in-plane magnetic field, the particle shows a sawtooth-like pattern of angle as a function of time, see Fig. S2. The aim is to obtain the torsion constant of the molecular complex from the measured pattern.

The oscillatory behaviour can be described[3] in terms of the applied magnetic field B, the effective magnetic moment of the particle m, the angle of excursion of the particle θ_p, and the angular velocity of the particle $\frac{d\theta_p}{dt}$:

$$\tau_m(B,m,\theta_{field},\theta_p) = \tau_{mol}(\theta_p) + \tau_{drag}(\frac{d\theta_p}{dt}) \qquad (1)$$

The term on the left corresponds to the applied magnetic torque τ_m. The terms on the right correspond to the nanomechanical torque of the protein complex under torsional deformation τ_{mol} and to the hydrodynamic drag τ_{drag}. In a continuously rotating magnetic field, the observed oscillatory behaviour at twice the frequency of the applied field is caused by remagnetization of the superparamagnetic particle.[3]

There are three torques acting in the system: the magnetic torque, the torque due to torsional strain in the protein complex, and the hydrodynamic torque due to the viscous medium:

$$m_{eff}Bsin(\varphi) = k(\theta_b)\theta_b + 8\pi C\eta R^3\frac{d\theta_b}{dt} \qquad (2)$$

C is a dimensionless factor that corrects for the hydrodynamic influence of the nearby substrate (which was estimated to be 1.22 for an M-270 particle), η is the dynamic viscosity of water ($1 \times 10^{-3}\, Pa \cdot s$), and *R* is the radius of the particle (1.4 µm). The hydrodynamic torque is included in the description, but it plays a negligible role in the experiments of this paper, since it is at least 10 times smaller than the other torques. The applied magnetic torque equals the product of the effective magnetic moment of the particle m_{eff}, the magnetic field *B*, and the angle φ between the direction of the field and the effective magnetic moment of the particle. The effective moment m_{eff} results from the presence of many magnetic crystals within the polymer matrix of the particle. We have developed a model in which the magnetism of the particle is described by *n* individual magnetic moments with an angular distribution (Gaussian, with spread σ_{angle}) and a distribution of coercivity (Gaussian, with mean B_c and spread σ_{B_c}).[6] The sawtooth-like pattern of angle as a function of time results from magnetic switching of the crystals due to the fact that the applied magnetic field is larger than the coercive field of the crystals. This switching underlies the fact that the sawtooth-like pattern has a frequency that is twice the frequency of the rotating field.[7] θ_b is the angle of the particle with respect to the equilibrium position when no torque is applied. The molecular torque is described as a Hookean angular spring with an angle-dependent torsion constant *k*. Eq. 2 was numerically solved using the Runge-Kutta method in Matlab.

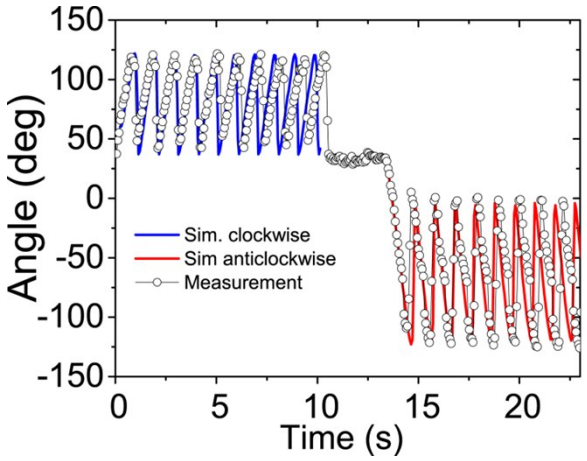

Figure S2 . *Experimental data (open circles) and simulation (red and blue lines) of a particle bound by the H4-H1 configuration. The particle is modelled by a distribution of magnetic grains with different coercivities. The used parameters are: magnetic moment* $m = 7.5 \times 10^{-17} Am^2$*, applied magnetic field* B*= 20 mT; frequency of rotation f = 0.5 Hz; mean coercive field* B_c*= 13 mT; spread of the coercive field* σ_{B_c}*= 2 mT; number of grains n=30; angular spread* $\sigma_{angle} = 90^o$*. Torsion constant for clockwise deformation (blue line)* $k = 3.4 \times 10^{-18} Nm/rad$*; torsion constant for anticlockwise deformation (red line)* $k = 1.3 \times 10^{-18} Nm/rad$*;*

Figure S2 shows a good agreement between the simulation and the measurement. In the simulations different torsion constants were used for clockwise and anticlockwise deformation, which points to a non-symmetric torsional profile of the molecular spring.

S4. Motion blur correction of ABM data

There are two artifacts that have to be taken into account when analyzing the ABM data. The first is the error made by the tracking software, the second is the motion blurring. The error made by the tracking software increases the width of the distribution, effectively giving a lower value of the spring constant. Typically the detection error is small (0.2 deg) compared to the total width of the distribution (5-10 deg) and can therefore be neglected. The other artifact, motion blurring, is caused by the relatively long exposure time of the camera compared to the instantaneous motion of the particle. Typically an exposure time of 50 ms (20 fps) is used. The detected position of the particle is the average position during this time, leading to an underestimation of the true width of the angular distribution and thus to an overestimation of the torsional spring constant. This effect gets more pronounced for larger spring constants. For our system the motion blur starts to play a significant role for spring constants above 10^{-18} Nm/rad. It is possible to correct for the motion blur.[7] According to the proposed theory the real variance of the distribution can be found via:

$$\mathrm{Var}(X) = \frac{\mathrm{Var}(\overline{X})}{S(W,k,f_r)}, \tag{3}$$

where $S(W,k,f_r)$ given by,

$$S(W,k,f_r) = \frac{f_r}{Wk} - \left(\frac{f_r}{Wk}\right)^2\left(1 - \exp\left(-\frac{Wk}{f_r}\right)\right), \tag{4}$$

with W the exposure time of the camera, k the true torsional spring constant, and f_r the rotational hydrodynamic drag. The true value of the torsional spring constant can be retrieved by assuming that the true variance is that of a thermally actuated harmonic torsional spring,

$$\mathrm{Var}(\overline{X}) = \frac{k_b T}{k}, \tag{5}$$

and using this equation to solve equation (3) for k. The equation is solved numerically using a Newton-Rapson method. The slope of equation (3) becomes shallow (i.e. does not depend strongly on k) around the solution, which can give instabilities. We therefore ensured that the blur corrected spring constant gives a variance that is an overestimation of k while trying to satisfy equation (3).

S5. Calcium concentration measurements

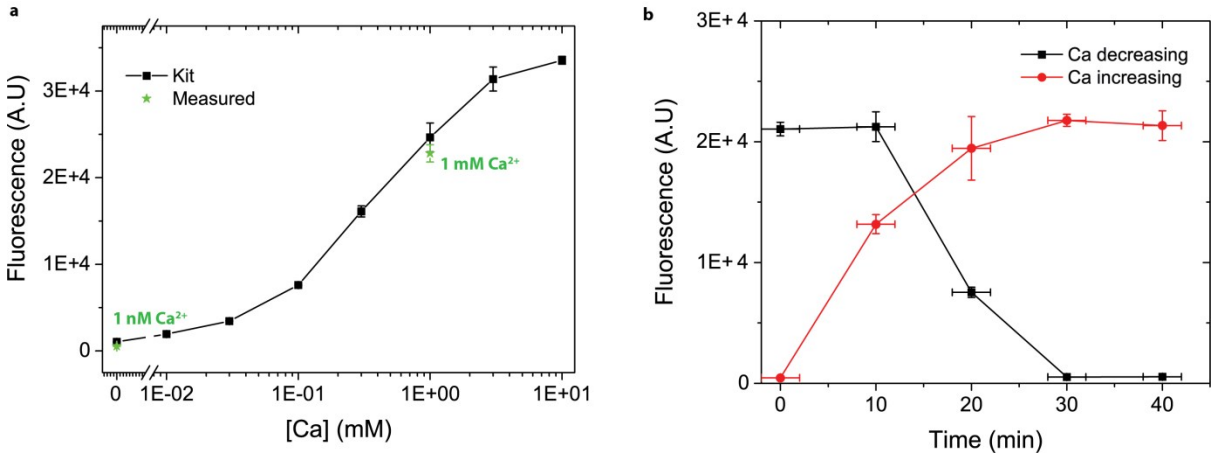

Figure S3 ***a.*** *Calcium assay fluorescence signals measured on the prepared calcium buffers (1 nM and 1 mM) and on the standard test templates provided in the kit.* ***b.*** *Ca^{2+} assay signal measured on the outlet fluid as a function of perfusion time. The red dots indicate an increase of the Ca^{2+} concentration from 1 nM to 1 mM, the black line indicate a decrease of the Ca^{2+} concentration from 1 mM to 1 nM.*

A flow cell was used in our experiments to vary the Ca^{2+} concentration. The outlet of the flow cell is connected to a reservoir where the remnant fluid was collected. A pump was connected to the inlet of the flow cell and the fluid with a given concentration of Ca^{2+} was pumped at a rate of 20 μl/min. Solutions with 1 nM and 1 mM free Ca^{2+} were prepared with EGTA according to the software Maxchelator.[8] To assess the concentration of calcium in the assay chamber, a fluorometric quantitative Ca^{2+} assay kit was used (Abcam, ab112115), see Figure S3a. The data show that the 1 mM Ca^{2+} is in good agreement with the 1 mM standard from the kit. Since the limit of detection of the kit is 0.03 mM Ca^{2+}, the 1 nM concentration could not be determined precisely; the 1 nM buffer corresponded to the negative control of the kit. Furthermore, the Ca^{2+} level in the flow cell was measured as a function of time, see Figure S3b. Samples of $\sim 200\ \mu l$ where were collected from the outlet reservoir of the chamber every 10 minutes. From the collected samples, 50 μl was used to measure the Ca^{2+} concentration according to the manufacturer's specifications. The fluorescence signal of the calcium assay was measured for the samples obtained at different instants of perfusion time. It was found that the waiting time required to obtain the desired calcium concentration inside the fluid cell was about 30 minutes.

S6. Calcium dependence of the H2-H1 system

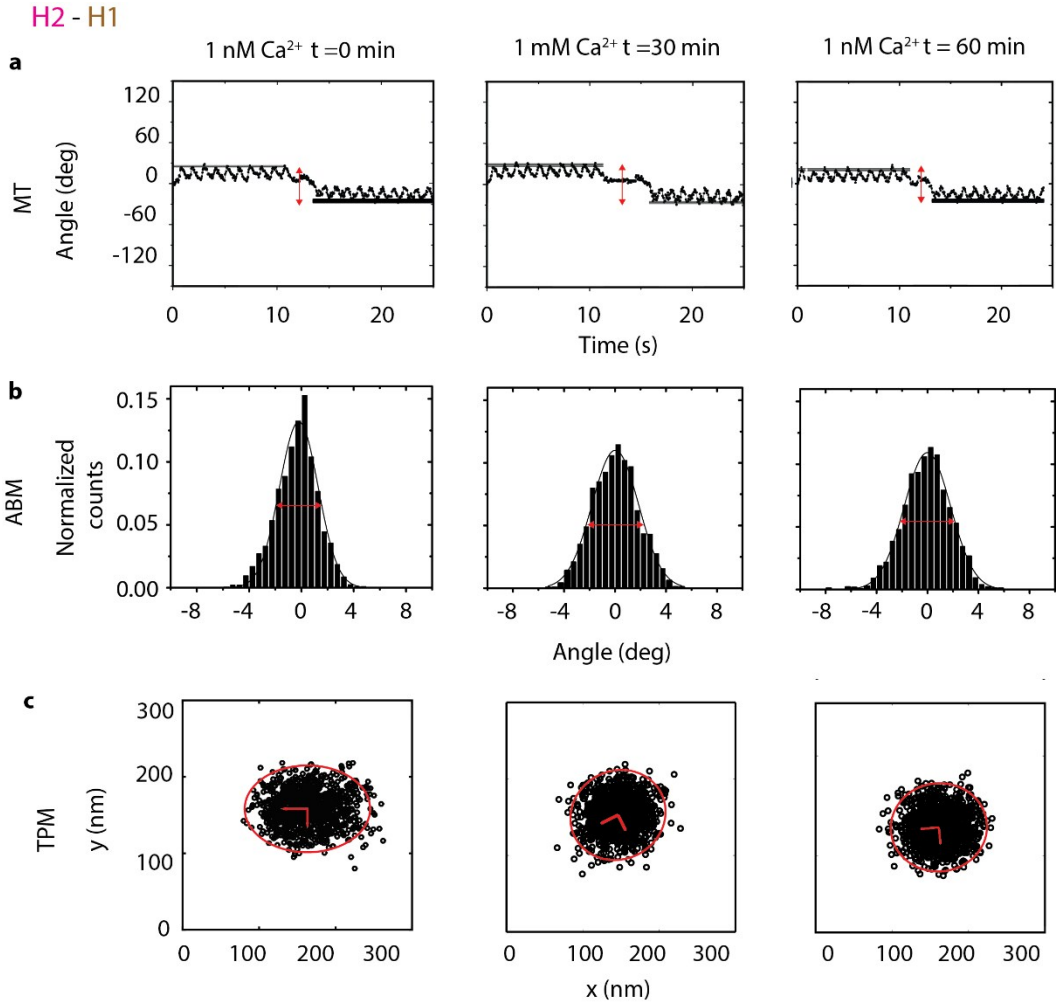

Figure S4. *Calcium dependence for a particle bound through the H2-H1 configuration. The initial Ca^{2+}concentration was 1 nM. Thereafter the Ca^{2+}concentration was increased in the fluid cell to 1 mM Ca^{2+}, and subsequently the Ca^{2+}concentration was reduced to 1 nM. At each concentration data was collected by the three measurement modalities:* ***a.*** *the angular deformation by MT experiments,* ***b.*** *the angular deformation by ABM, and the* ***c.*** *the Area by TPM measurements. Measurements at each Ca^{2+} concentration have a time difference of* $\sim 30\ min$.

S7. Origin of the variabilities in torsion constants

The observed spread in the torsion constants can have different origins. The cTn complex itself may be a source of variability. The cTn complex consists of I, C and T subunits (see Fig. 1a). The material as supplied by the manufacturer contains cTnI : cTnT : cTnC at a nonstoichiometric ratio of 1 : 0.68 : 1.10, which means that not all cTn complexes are in the form of the complete heterotrimer. Some complexes may for example lack the cTnT subunit and thereby exhibit a larger flexibility.

In the MT measurements the magnetic properties of the particles contribute to variability. The maximum angle of deformation is derived from the condition of maximum torque, which depends on the maximum torque that can be applied by the magnetic particle, which has a variability of about 28% for the M-270 particles[3].

The antibody coupling procedures (EDC-NHS conjugation on the particle, physisorption on the substrate) used in the experiments are non-directional. A variability of antibody orientation can have a direct as well as an indirect influence on the nanomechanical observables. The direct effect results from the nanomechanical flexibility of the antibody itself. An upper limit of the absolute direct contribution of the antibodies to the measured flexibility parameters can be estimated by the signals measured on the stiffest antibody-cTn-antibody system, i.e. the H2-H1 configuration. The H2-H1 experiment yields smaller flexibility parameters than the H4-H1 experiment (see Table S1) and indicates that the direct contribution of the antibodies is not dominant in the H4-H1 data. Previous measurements on a system containing one antibody (Protein G-IgG) exhibited variations of torsion angle of 30%, and systems with two antibodies (IgG-IgG) showed 40% of variation[3].

The antibodies may also indirectly contribute to variability, by influencing the orientation of the sandwiched cTn complex with respect to the symmetry axis of the particle-substrate system. Since the torsional measurement methods record in-plane rotational motion of the particle, with the rotation axis normal to the surface, the observed torsional stiffness is expected to depend on the orientation of the cTn complex with respect to the axis of rotation. In future research it will be interesting to study the role of antibody directionality and to investigate also other epitope binders such as Fab fragments, nanobodies and aptamers.

References

1. Gutiérrez-Mejía, F. A., van IJzendoorn, L. J. & Prins, M. W. J. Surfactants modify the torsion properties of proteins: A single molecule study. *N. Biotechnol.* 32, 441–449 (2015).

2. Janssen, X. J. A. *et al.* Torsion stiffness of a protein pair determined by magnetic particles. *Biophys. J.* **100,** 2262–7 (2011).

3. Van Reenen, A., Gutiérrez-Mejía, F. A., Van IJzendoorn, L. J. & Prins, M. W. J. Torsion profiling of proteins using magnetic particles. *Biophys. J.* **104,** 1073–1080 (2013).

4. Jacob, A., van IJzendoorn, L. J., de Jong, A. M. & Prins, M. W. J. Quantification of protein-ligand dissociation kinetics in heterogeneous affinity assays. *Anal. Chem.* 84, 9287–94 (2012).

5. Dorokhin, D. et al. Molecular interference in antibody-antigen interaction studied with magnetic force immunoassay. *N. Biotechnol.* 32, 450–7 (2015).

6. Gutierrez Mejia, F.A., Proteins with a twist: torsion profiling of proteins at the single molecule level. Ph.D. thesis, Eindhoven University of Technology, 2016, pp 15-32

7. Wong, W. P. & Halvorsen, K. The effect of integration time on fluctuation measurements: calibrating an optical trap in the presence of motion blur. Opt. Express 14, 12517 (2006).

8. Ca-EGTA Calculator TS v1.3: https://web.stanford.edu/~cpatton/CaEGTA-TS.htm